Metallography, Microstructure, and Analysis (2020) 9:312–322
https://doi.org/10.1007/s13632-020-00639-0

TECHNICAL ARTICLE

Effect of Heat Treatment on Microstructure and Properties of Al-7.0Zn-1.5Cu-1.5Mg-0.1Zr-0.1Ce Alloy

Jinhua Chu[1] · Ting Lin[1] · Guojing Wang[2] · Hongjie Fang[1,3] · Diangang Wang[3]

Received: 16 May 2019 / Revised: 21 February 2020 / Accepted: 7 April 2020 / Published online: 27 April 2020

Abstract

To obtain excellent properties in 7××× series aluminum alloys, the heat treatment process used is an important factor. This needs to be chosen according to the different alloy compositions. A 7××× series aluminum alloy with high zinc content (Zn/Mg > 4, Mg/Cu = 1) was prepared. Studying the heat treatment process of the alloy is important to guide companies in its industrial production. The optimum heat treatment process is explored from a microstructure point of view. The alloy was melted and cast in the laboratory using a metallurgical method. The microstructure, fracture morphology, and mechanical properties of the alloy were examined by metallographic microscopy, scanning electron microscopy, transmission electron microscopy (TEM), and tensile testing. Research on the alloy solution treatment was emphasized. The results showed that the solution effect was optimum at 470 °C × 1 h during a single-stage solution treatment. The recrystallization degree was low when the two-stage solution treatment process was 450 °C × 0.5 h + 475 °C × 0.5 h due to the release of deformation energy at low temperature; at the same time, the second-order solid-solution temperature was high, the solid-solution effect was better than in the single-stage solid-solution treatment, and the comprehensive mechanical properties of the alloy were better.

Keywords 7××× Series aluminum alloy · Solution treatment · Homogenization heat treatment · Microalloying element

Introduction

Al-Zn-Mg-Cu alloys belongs to the 7××× series of ultra-high-strength/toughness aluminum alloys, being widely used in the aerospace, high-speed trains, and other transportation fields due to their low density, high specific strength, high hardness, prefect processing performance, and excellent corrosion resistance [1–4]. Such 7××× series aluminum alloys are easy to produce by component segregation in melting and casting due to their complex composition and high content of alloy element [5–7]. Moreover, 7××× series aluminum alloys belong to the heat-treatable strengthening aluminum alloys. Nanosized strengthening phases such as η are precipitated in the crystal, and the mechanical properties of the alloy are improved by solution aging treatment [8–11]. In terms of adding alloying elements, addition of trace transition-group and rare-earth elements can have a favorable effect on 7××× series aluminum alloys [12, 13]. Al-Zn-Mg-Cu wrought alloys are commonly formed by a wrought manufacture process such as equal-channel angular pressing (ECAP), severe plastic deformation (SPD), cryorolling, or other controlled thermomechanical treatment (TMT), resulting in especially excellent mechanical properties [14, 15].

The strengthening effect of heat treatment on 7××× series aluminum alloys mainly depends on the amount of precipitation of η and η′; therefore, the solid solution treatment system is very important for the subsequent aging treatment. The solid-solution treatment mainly involves dissolving the coarse second phase of the alloy into the matrix followed by the formation of a supersaturated solid solution during rapid cooling. It is well known that undissolved coarse

✉ Hongjie Fang
h.j.fang@163.com

Jinhua Chu
104052574@qq.com

Ting Lin
517817900@qq.com

Guojing Wang
412404460@qq.com

[1] Department of Material Science and Engineering, Yantai Nanshan University, Yantai 265713, China

[2] Shandong Drug and Food Vocational College, Weihai 264210, China

[3] Shandong University, Jinan 250100, China

intermetallic phases are detrimental to the mechanical properties, especially toughness [16–19]. Therefore, the main purpose of studying the solid-solution treatment system is to make the coarse second phase dissolve into the matrix as much as possible and to increase the volume fraction of the effective precipitated phase.

Scholars have carried out much research work in the field of heat treatment systems [20–22]. However, different heat treatment processes should be adopted for different main elements. On the basis of other scholars' research, the present study considers a kind of high-Zn aluminum alloy, which reduces the content of Cu and Mg, increases the ratio of Zn/Mg, and adds trace rare earth Ce. An aluminum alloy sheet was prepared in the laboratory, and research work on the solid-solution treatment system of the alloy was carried out, thereby accumulating experience for further research on heat treatment processes.

Experimental Materials and Procedures

Experimental Materials and Chemical Reagents

Pure aluminum (99.85%), pure zinc (99.9%), pure magnesium (99.9%), Al-Cu alloy (20%), Al-Zr alloy (10%), Al-Ce alloy (10%), C_2Cl_6 (analytical reagent), NaCl (analytical reagent), KCl (analytical reagent), and Na_3AlF_6 (analytical reagent) were used in the present work.

Experimental Equipment and Tools

A well-type crucible furnace (SG2-5-10), a box-type resistance furnace (SX2-12-10), a drying oven (101A-00), a metallographic microscope (Axio Imager M2m), a transmission electron microscope (Nova-NanoSEM450), a differential scanning calorimeter (DSC1), a hot rolling mill ($\Phi 200 \times 350$), a cold rolling mill ($\Phi 75 \times 300$), a polisher (P-2T), a pointing machine (Opal400), a BROVICK hardness gauge (HBRV-187.5), an electronic universal testing machine (WDW-T100), an ICP-MS (Nexion 300) graphite crucible, a mold, a bell, and a sludge ladle were used in the present work.

Experimental Process

The experimental materials were taken according to the nominal compositions presented in Table 1. A well-type crucible furnace was used for smelting. During smelting, pure aluminum and intermediate alloy were put into graphite crucible, and a small amount of covering agent (NaCl, KCl, and Na_3AlF_6 in a proportion of 2:2:1) was added. The temperature was raised to 780 °C and held for at least 15 min. After the melting of the experimental materials, mixing, degassing, and slagging-off were carried out, and the covering agent was then applied. When the temperature dropped to 730 °C, pure zinc and magnesium were added, and pure magnesium was calculated according to a 5% burnout rate. Considering the low density and flammability of pure magnesium, this was pressed into the bottom of the liquid using a bell. Once all the pure magnesium had melted, mixing, degassing, slagging-off, and stationary were carried out. When the temperature dropped to 720 °C, pouring began. An aluminum alloy slab ingot with dimensions of 200 mm × 120 mm × 20 mm was cast in the mold.

The cast aluminum alloy slab ingot was obtained after a homogenized annealing process in a box-type resistance furnace. As in previous literature [23], the annealing process was 455 °C × 12 h + 475 °C × 12 h. After homogenized annealing, the actual chemical elements in the aluminum alloy slab ingot were measured by inductively coupled plasma (ICP) analysis. The results are presented in Table 1. Aluminum alloy sheets 4 mm thick were prepared using a hot rolling mill. The starting rolling temperature was 440 °C. Each screw-down amount was 1–2 mm; annealing was carried out in the middle, and the total deformation was 80%. The hot-rolled sheets were then submit to recrystallization annealing at 440 °C × 3 h and air-cooling. Sheets 2 mm thick were prepared using the cold rolling mill with deformation of 50%.

The cold-rolled aluminum alloy sheets were treated by solution aging. The single-stage solution temperature was 460, 470, and 480 °C. The holding time was 30 min, 60 min, and 120 min, respectively. The aging temperature was 120 °C. The holding time was determined using a hardness test according to one of the solution temperatures. Aluminum alloy sheets that were treated with solution aging were processed into standard samples to study their mechanical properties, optimum temperature, and holding time of single-stage solution treatment. The mechanical properties were measured using an electronic universal testing machine (WDW-T100); the gauge length of the test specimens was 55 × 8 mm, and the stretching speed was 1 mm/min; the average value of three samples was taken. According to the optimum technological parameters of the single-stage solution

Table 1 Nominal composition ratio of alloys (mass fraction %)

	Zn	Cu	Mg	Zr	Ce	Al
Nominal composition	7.0	1.5	1.5	0.1	0.1	Bal.
Actual composition	7.06	1.48	1.51	0.12	0.09	Bal.

treatment, the two-stage solution treatment was formulated and the mechanical properties were tested.

The as-cast structures, homogeneous states, and solution-treated microstructures were observed by metallographic microscopy. The eutectic point of the as-cast alloys was measured using differential scanning calorimetry, providing a reference for the formulation the homogenization annealing and solution treatment of the as-cast alloys. Phase analysis of the as-cast alloys was carried out by x-ray diffraction (XRD) analysis. The fracture morphology was analyzed by field-emission scanning electron microscopy. The grain interior precipitated phases of the alloy after solution aging were analyzed by transmission electron microscopy.

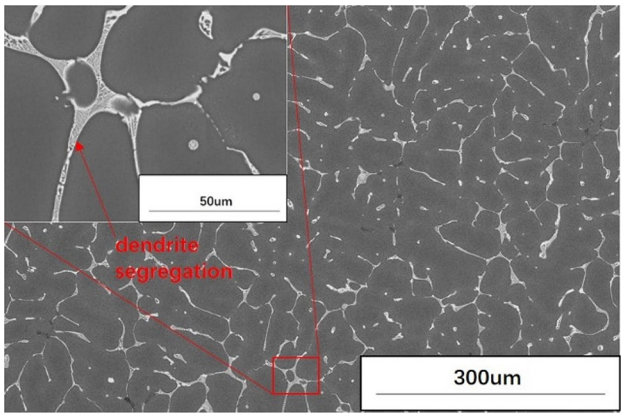

Fig. 2 Microstructure of as-cast alloy under scanning electron microscopy

Results

Microstructure of As-Cast Alloys

Cast aluminum alloys were mounted, roughly ground, finely ground, and mechanically polished. These were then anodized, and their metallographic structure was observed under a metallographic microscope. The as-cast structure showed a typical dendritic structure, as shown in Fig. 1. Dendrite segregation is evident at grain boundaries. Due to the presence of Zr and Ce in the alloy composition, the secondary dendrite space can be reduced by refining grains in the alloy melting. Another reason is that alloys have many kinds of high-content and easy-to-form eutectic compounds with a low melting point at grain boundaries. The as-cast structure was observed by scanning electron microscopy. Dendrite segregation at the grain boundary was obvious, as shown in Fig. 2, where eutectic compounds with high brittleness and low melting point were easily formed. Therefore, it was necessary to apply follow-up homogenization annealing to eliminate dendrite segregation as far as possible, improve the plasticity of the alloy, and prepare for subsequent plastic processing.

Microstructure of Homogeneous States of Alloys

The lowest melting point of the as-cast alloys was measured using a differential scanning calorimeter (DSC-800). As shown in Fig. 3, there are two endothermic peaks. The first endothermic peak occurred at 474.48 °C, proving the presence of a low-melting-point alloy at this temperature, and the low-melting-point phase began to melt. The second endothermic peak of 484.91 °C was higher and absorbed more heat, proving that the alloy melted at this temperature. Therefore, the subsequent single homogenization process and single-stage solution treatment cannot exceed the first peak value. Also, the first heating temperature of the two-stage homogenization process and two-stage solution treatment should not exceed the first peak value. The

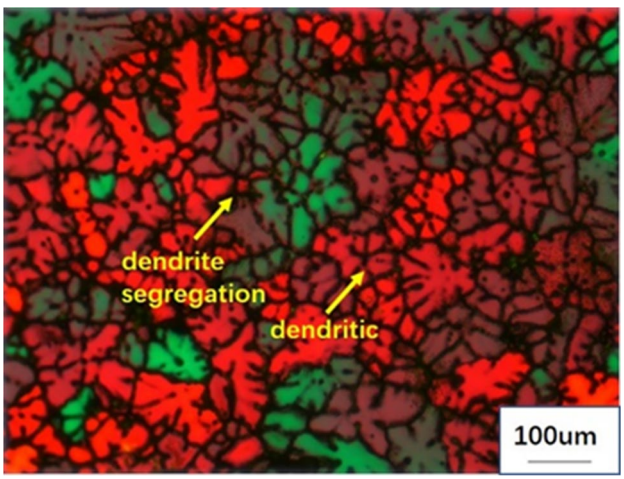

Fig. 1 Metallographic structure of as-cast alloy

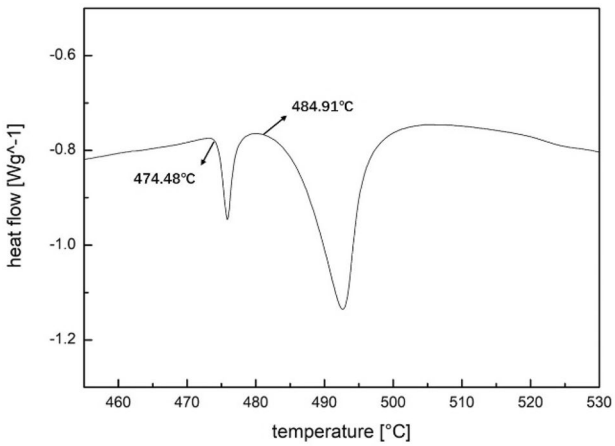

Fig. 3 DSC curves of alloy

second-stage heating temperature can try to slightly exceed the first peak, but it must not exceed the second peak temperature, otherwise it will cause overburn.

The homogenizing treatment was formulated according to literature [23]. Two-stage homogenization annealing of 455 °C × 12 h + 475 °C × 12 h was adopted. The microstructure of the homogenized alloy was observed using a metallographic microscope. As shown in Fig. 4, the dendrite segregation disappeared at the grain boundary of the alloy, and the boundary between the grains was only seen as a shallow line. Some of the grain boundaries were discontinuous and showed good homogenization results.

Mechanical Properties of Alloy

Study on Single-Stage Solution Treatment Technology

Several samples with dimensions of 100 mm × 16 mm were prepared from the 2-mm cold-rolled sheet using a shearing machine. Solution treatment and water-cooling were carried out in a salt bath furnace. The durationb of sample transfer from the furnace to water was not longer than 10 s. Aging treatment at 120 °C × 24 h was completed in the drying oven after solution.

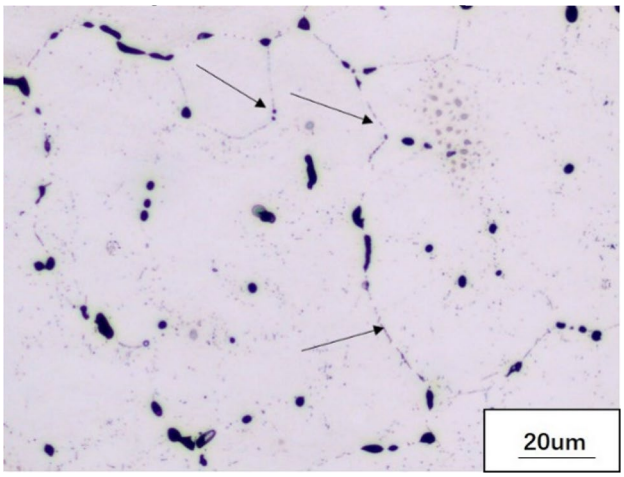

Fig. 4 Metallographic structure of alloy after homogenization

This experiment studied mainly the single-stage solution treatment. The solution treatment temperature was based on the minimum melting point temperature of the as-cast aluminum alloy as measured by the differential scanning calorimeter. As shown in Fig. 3, the first endothermic peak occurred at 474.48 °C. The first solid-solution treatment temperature was determined to be 470 °C; on based on this temperature, the temperatures of the other solid-solution treatments could then be determined with a 10°C increase or decrease, giving solution treatment temperatures of 460 °C, 470 °C, and 480 °C. The holding time takes into account the alloy composition (high content of alloy component), sheet thickness (2 mm), and heating conditions (air furnace). At the same time, according to literature [24], the holding time at each temperature was 0.5, 1, and 2 h, respectively. Three samples were taken from each group, and the average value was measured.

The results of the mechanical properties tests are presented in Table 2. The tensile strength and yield strength of the alloy gradually increased with prolongation of the holding time when the solution temperature was 460 °C. Among them, the mechanical properties of the alloy were the best when the holding time was 2 h. When the solution treatment temperature was 470 °C, the yield strength and tensile strength exhibited a rise and then a decrease with increasing holding time. At this time, the elongation values changed little. The comprehensive properties of the alloy were best when the holding time was 1 h. The yield strength, tensile strength, and elongation of the alloy began to decrease when the solution temperature was 480 °C. Comparing with the solution temperature, the comprehensive properties were the best at 470 °C, followed by 460 °C, and worst at 480 °C. These results show that the single-stage solution treatment at 470 °C × 60 min is the best process for the alloy.

Table 2 Results of mechanical tests on alloys

Solution treatment temperature (°C)	Holding time, min	Yield strength, MPa	Error, MPa	Tensile strength, MPa	Error, MPa	Elongation, %	Error, %
460	30	498	±5	529	±5.3	12.56	±0.13
	60	500	±5	533	±5.3	11.83	±0.12
	120	503	±5	542	±5.4	11.28	±0.11
470	30	509	±5.1	555	±5.6	13.01	±0.13
	60	527	±5.3	579	±5.8	12.45	±0.12
	120	512	±5.1	565	±5.7	12.85	±0.13
480	30	486	±4.9	532	±5.3	10.17	±0.1
	60	479	±4.8	519	±5.2	9.52	±0.1
	120	452	±4.5	501	±5	8.92	±0.09

Determination of Aging Time

The heat treatment system chosen for this experiment was aging treatment after solution treatment. The solution treatment used to determine the holding time for aging was 470 °C × 1 h. The aging temperature was 120 °C, and 18 small samples with dimensions of 15 mm × 15 mm were taken. After the solution treatment, the small samples were put into the drying oven to maintain a constant temperature. The holding times of the 18 small samples were 2, 4, 6, and 36 h. The Vickers hardness of the small sample was tested with a hardness gauge after aging. The age hardening curve is shown in Fig. 5. With prolongation of aging and holding time, the hardness of the alloy exhibited a sudden rise then increased slowly. The hardness reached its maximum when the holding time was 24 h. The hardness was determined to be 206.13 HV. After 24 h, the hardness decreased slowly. After 32 h, the descent rate accelerated. The aging process of this experiment was determined to be 120 °C × 24 h based on literature [25].

Mechanical Properties after Two-Stage Solution Treatment

The phase diagrams associated with Al alloys reveal that, the higher the temperature, the higher the solubility and the better the solution effect. Therefore, on the basis of the single-stage solution treatments, the two-stage solution treatment was studied. The solution temperature and solubility can be increased as much as possible so as to further achieve a better solution effect and improve the mechanical properties of the alloy. According to Ref. [26], combined with the single-stage solution treatment, the two-stage solution treatment was set at 450 °C × 0.5 h + 475 °C × 0.5 h. Moreover, this was compared with the single-stage solution treatment on the above basis.

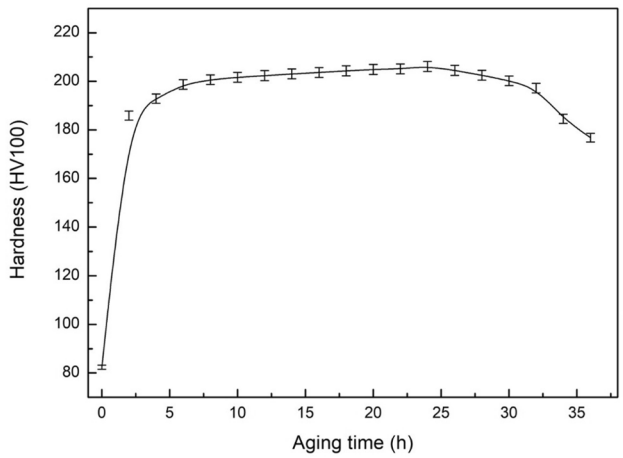

Fig. 5 Age-hardening curve of alloy

After the two-stage solution treatment, the aluminum alloy sheets were treated by artificial aging at 120 °C × 24 h, then processed into standard samples. The mechanical properties were measured on an electronic universal testing machine. The yield strength, tensile strength, and elongation resulted as 565, 594 MPa, and 12.95%, respectively. The comprehensive mechanical properties were obviously improved compared with those resulting from the single-stage solution treatment at 470 °C × 1 h.

Comparison of Metallurgical Structure of Alloys after Solution

The three samples with the best comprehensive mechanical properties after single-stage solution treatment at different temperatures were selected. After grinding and polishing, these samples were observed using a metallographic microscope. The metallographic structure after two-stage solution treatment was compared and analyzed. Figure 6 shows that the alloy sheet obviously recrystallized when the alloy was treated at 460 °C × 2 h. Moreover, most of the grains were elongated. However, the content of the second phase was too high to be fully dissolved in the matrix. This would also lead to insufficient solubility. When the alloy was treated at 470 °C × 1 h, most of the second phase of the alloy was dissolved in the matrix. Unfortunately, recrystallization occurred in the alloy sheets. When the alloy was treated at 480 °C × 0.5 h, the second phase was dissolved in the matrix, so less residual was found. However, it appears that most of the alloys were recrystallized, and even the grains grew. This would cause the mechanical properties of the alloy to decline. When the two-stage solution treatment process at 450 °C × 0.5 h + 475 °C × 0.5 h was adopted, only a small amount of recrystallization occurred at a few locations in the alloy. Moreover, most of the second phase dissolved into the matrix, and only a small amount of residual second phase was distributed among the grains.

Analysis of Fracture Morphology of Alloys

The fracture morphology of the tested specimens was observed by scanning electron microscopy. As shown in Fig. 7, when the alloy sheet was solution aged at 460 °C × 2 h, a large number of dimples were distributed on the fracture surface. Moreover, the alloy showed good toughness. The main fracture mode was transcrystalline rupture. Only a few locations presented intergranular fracture, which may be due to the presence of a coarse second phase, where cracks break along the grain boundaries of the second phase and the matrix. When the alloy sheet was solution aged at 470 °C × 1 h, the fracture morphology showed a distribution of a large number of dimples, which appeared to be deeper. Moreover, intergranular fracture characteristics were not found, so the toughness of the alloy can be

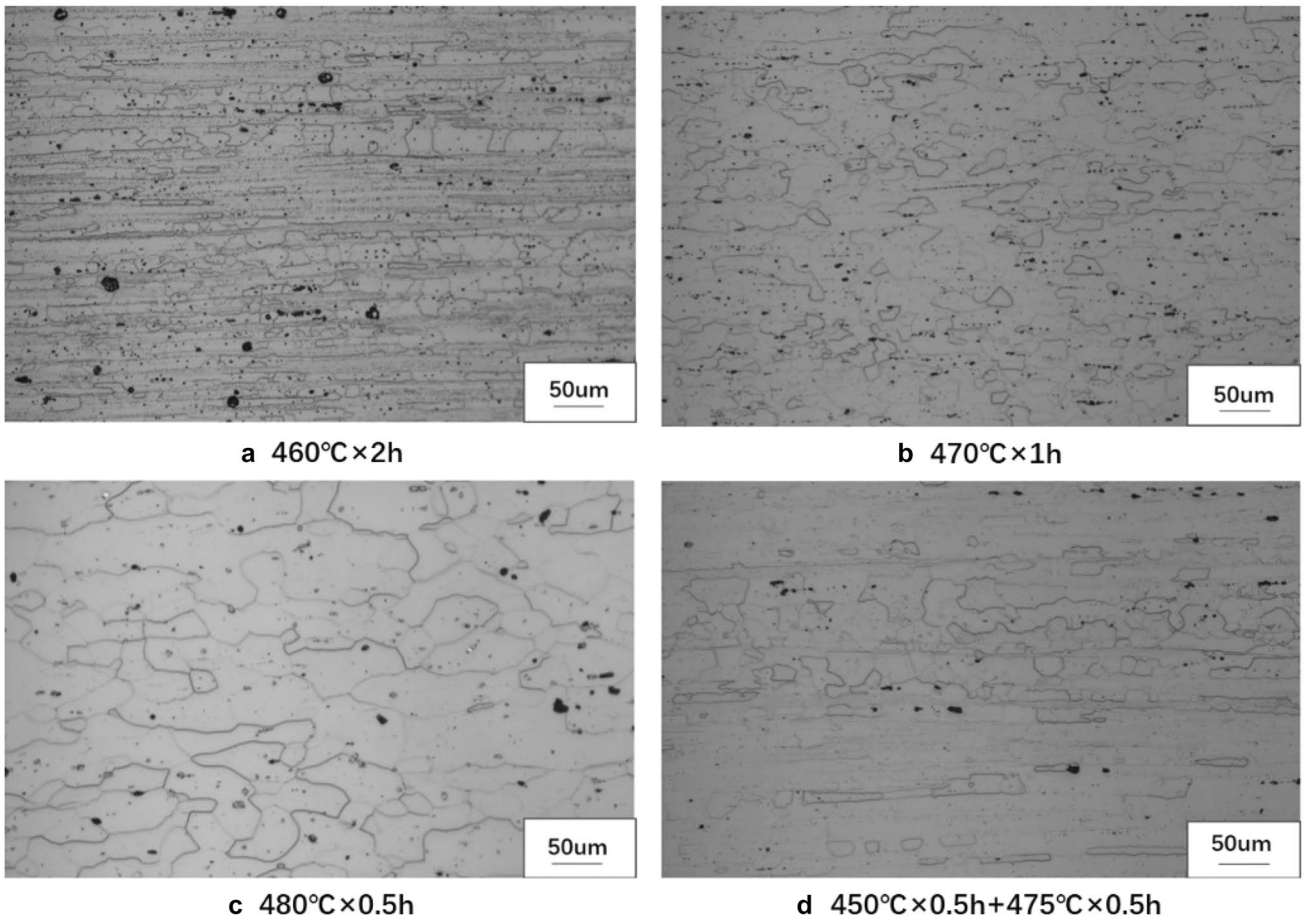

Fig. 6 Comparison of metallographic structure of alloy treated by solution treatment

judged to be better. When the alloy sheet was solution aged at 480 °C × 0.5 h, the fracture morphology showed less dimples, and the grain size was obviously coarse. Besides, a large number of intergranular fracture structures with smooth fracture surface and brittle fracture characteristics appeared, confirming the poor toughness and mechanical properties. The reason for this may be that the temperature was too high, resulting in grain growth. Furthermore, due to the complex composition of the alloy, low-melting-point phases appeared at individual locations. This is due to overburning, resulting in brittle fracture. When the alloy sheet was solution aged at 450 °C × 0.5 h + 475 °C × 0.5 h, a large number of dimples appeared in the fracture morphology. On the fracture surface, the grains were smaller and the dimples were deeper. Mainly transcrystalline rupture was observed, but no intergranular fracture.

Discussion

Analysis of Alloy Composition and As-Cast Microstructure

The main components of the designed 7××× series aluminum alloy are Zn with 7.0% content, followed by 1.5% Mg (with Zn/Mg > 4) and 1.5% Cu (with Cu/Mg = 1). There are also trace amounts of Zr and rare-earth Ce, both of which at 0.1%. In the solidification process of the alloy, unbalanced solidification occurred due to the faster cooling rate, which resulted in segregation. Therefore, there is a possibility of the occurrence of locally Cu-rich regions, which are prone to formation of Al_2Cu and

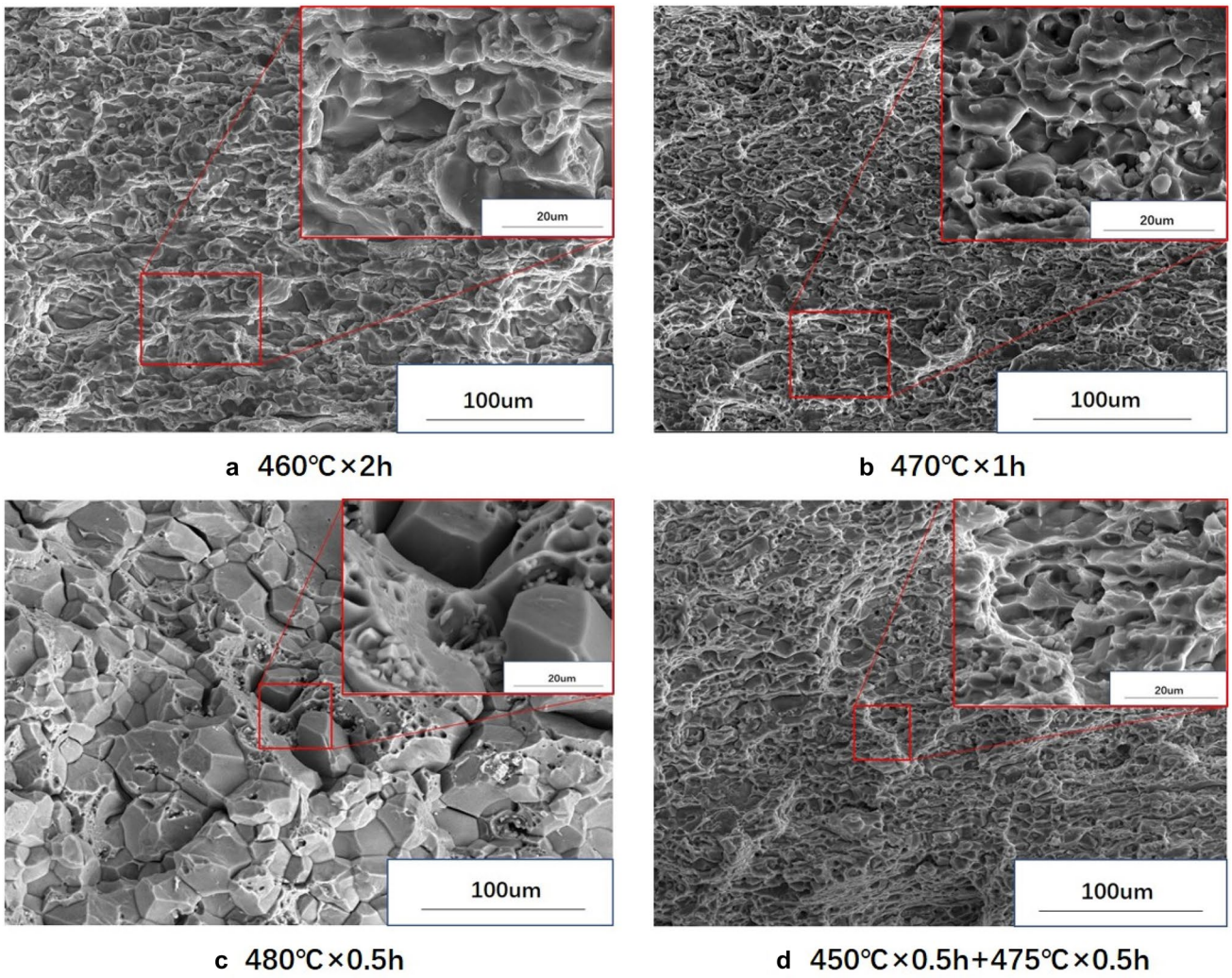

Fig. 7 Fracture morphology of alloy after solution aging treatment

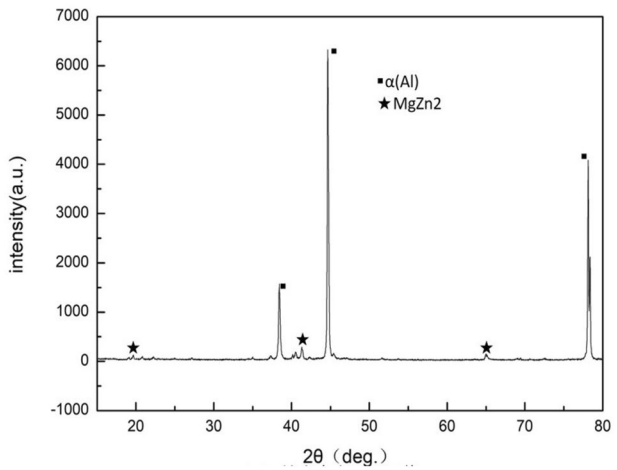

Fig. 8 XRD patterns of as-cast alloys

Al_2CuMg phases. However, the composition of the alloy is higher, and the content of Mg is only 1.5%. Another reason is that Mg preferentially forms nonequilibrium solidified $Mg(Al,Cu,Zn)_2$, so a large amount of Mg was consumed during solidification. Therefore, it was difficult to form S (Al_2CuMg) [27], even though there were locally Cu-rich regions. Phase analysis of as-cast alloys was carried out. As shown in Fig. 8, S (Al_2CuMg) and θ (Al_2Cu) phases were not found. Thus, it can be judged that the S and θ phases do not exist or have low content in as-cast alloys. The diffraction peaks are weak and not shown in the figure, so they can be neglected. The structure of $MgZn_2$ is the same as that of $Mg(Al,Cu,Zn)_2$, which can be understood as the formation of $Mg(Al,Cu,Zn)_2$ quaternary phase by solid solution of Al and Cu atoms into $MgZn_2$. It is only slightly offset from the original $MgZn_2$ peak, so the phase of the diffraction peak in Fig. 8 is actually $\alpha(Al) + Mg(Al,Cu,Zn)_2$.

The alloy contains trace element Zr, which can react with Al to form Al_3Zr. The lattice constant of Al_3Zr dispersed phase is 0.408 nm, while that of Al is 0.404 nm, so the Al_3Zr particles are coherent with the matrix according to metal solidification theory.

$$C_s = C_0\left[1-(1-k_0)\exp\left(-\frac{k_0 v}{D_L}x\right)\right],$$

where C_s is the solid solute concentration, C_0 is the average solute concentration, k_0 is the equilibrium distribution coefficient, v is the solidifying rate, and D_L is solute diffusion coefficient. The equilibrium distribution coefficient k_0 of Zr element is greater than 1. Therefore, during the solidification, Zr diffuses to the solid side and forms Al_3Zr in the intercrystal. The equilibrium distribution coefficient k_0 of the other alloying elements (such as Zn, Cu, Mg, and Ce) is less than 1, and these diffuse to liquid phase during solidification. Furthermore, the concentration of solute in liquid phase becomes higher and higher. Finally, segregation occurs at grain boundaries. Therefore, the dendrite segregation in the as-cast structure of the alloy is obvious, as shown in Fig. 2, and its subsequent homogenization annealing is very important.

Analysis on Heating Treatment of Alloys

According to homogenization theory, the relationship between diffusion coefficient and temperature is $D = D_0\exp(-\frac{Q}{RT})$, where D_0 is the diffusion constant, Q is the diffusion activation energy, R is the gas constant, and T is temperature. The relationship between the diffusion coefficient D and temperature T is exponential. The higher the temperature, the faster the diffusion. Therefore, increasing the homogenization temperature can not only improve the diffusion effect but also reduce the homogenization time. DSC was used to test the alloy. The endothermic peak appeared at 474.8 °C. To obtain a better homogenization effect, a two-stage homogenization process was adopted. The eutectic phase with low melting point would diffuse and dissolve into the matrix gradually at 455 °C. When the second homogenization temperature rose to 475 °C, no overburning phenomenon occurred, which is due to the diffusion of eutectic phase with low melting point. Also, as a consequence of this, the diffusion rate was accelerated, the dissolution of coarse second phase was promoted, and the homogenization effect was improved. As shown in Fig. 9, after homogenization, all the second phases except a small amount of coarse Fe-rich phase dissolved into the matrix by diffusion.

The mechanical properties of the alloy were controlled by two factors during the solution treatment. On the one hand, the recrystallization of cold-processed aluminum alloy

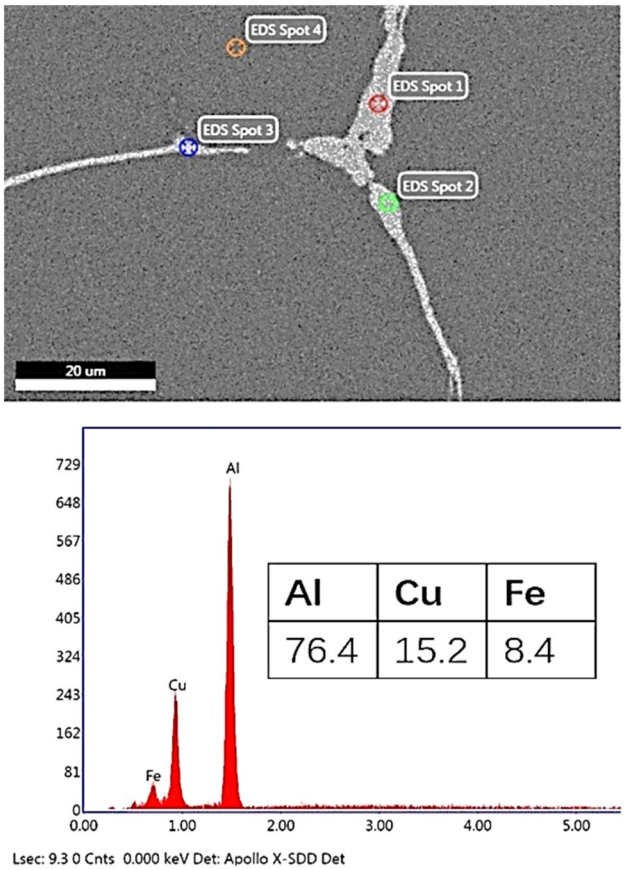

Fig. 9 Energy spectrum analysis of alloy after homogenization

sheets occurred when the heating temperature was increased and the holding time prolonged, resulting in a decrease in strength and an increase in plasticity. At the same time, the second-phase particles diffused into the matrix due to the increase in temperature and the prolongation of the holding time during the solution. The supersaturated solid solution was formed after quenching. This is conducive to the precipitation of fine secondary phases in the subsequent aging process, and improves the strength and toughness of the alloy. Therefore, the supersaturated solid solution at the initial stage of the solution treatment plays a major role in the mechanical properties. With the prolongation of the holding time, less and less alloying elements diffused into the matrix, while the recrystallization degree became higher and higher. Recrystallization plays a major role in affecting the mechanical properties. In this experiment, when the temperature of the single-stage solid solution treatment was 460 °C, the holding time was 2 h. The alloy sheet with the best comprehensive mechanical properties was obtained under these conditions. The best mechanical properties of the alloy sheet could be obtained with single-stage solution treatment at 470 °C and holding for 1 h. The alloy sheet with the best mechanical properties will be produced with a

temperature of 480 °C and holding time of 0.5 h, although the holding time will be gradually reduced with increasing solution temperature.

The main purpose of the two-stage solution treatment is to dissolve the nonequilibrium eutectic low-melting-point phase into the Al matrix by diffusion at low temperature. Then, the solid phase of the alloy is increased. The lowest temperature of the low-melting-point phase is higher than the second solution temperature, but this will not cause overburning. In this way, it can be ensured that the alloy will exhibit a better solid-solution effect at high temperature. Moreover, the coarse second phase can basically be eliminated and the comprehensive mechanical properties of the alloy can be improved. In addition, because plastic deformation occurs in the alloy sheet and a large amount of deformation energy is stored, the deformation energy will become the driving force for alloy recrystallization at a certain temperature. At low temperatures, the stored deformation can be released. The recovery action consumes part of the deformation energy, reduces the driving force of recrystallization, and reduces the percentage of recrystallization. The grain boundary migration rate V can be expressed through crystal boundary migration theory [28] as

$$V = FM, \tag{1}$$

$$F = P_{\mathrm{D}} - P_{\mathrm{Z}} - P_{\mathrm{SOL}}, \tag{2}$$

$$M = M_0 \exp\left(-\frac{Q}{RT}\right), \tag{3}$$

where F is the driving force, P_{D} is the stored deformation energy, P_{Z} is the obstruction effect of particles, P_{SOL} is the obstruction effect of solute atoms, M is the crystal boundary mobility rate, M_0 is a constant, Q is the activation energy, R is the gas constant, and T is absolute temperature. From this formula, it can be seen that the stored deformation energy can reduce the driving force for crystallization, thus reducing the crystal boundary migration rate. The degree of recrystallization also decreases. Ultimately, the recrystallized grain growth can be stunting. As seen from the metallographic diagram of the solution in Fig. 6, the second-stage temperature of the two-stage solution treatment is 475 °C. Although this temperature is not low, the corresponding recrystallization degree is lower than that of the single-stage solution treatment at 470 °C.

The high strength and toughness characteristics of 7××× series aluminum alloys mainly depend on precipitates in the intracrystalline and grain boundary. The purpose of solution is to increase the solubility. The alloy strength can be improved by increasing the number of precipitates. In this experiment, the medium-temperature aging treatment system at 120 °C was selected. The precipitation sequence

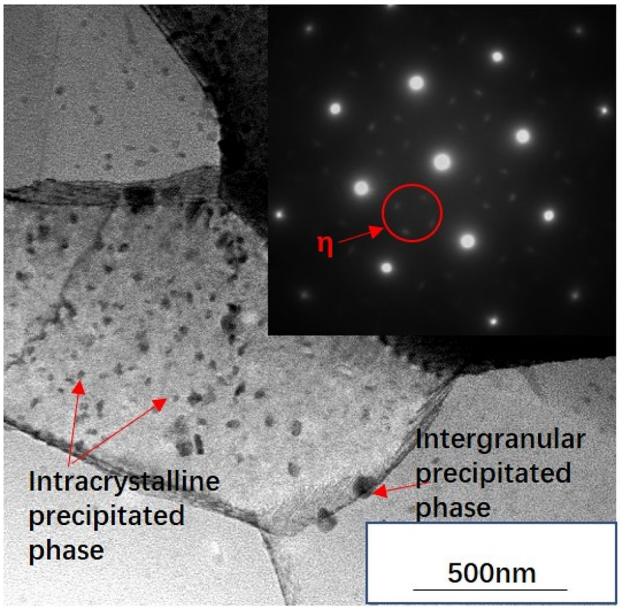

Fig. 10 TEM microstructure and corresponding diffraction patterns of alloy after solution aging treatment

is: supersaturated solid solution → Guinier–Preston (GP) region → η′ phase. To keep the strengthening phase in the GP region of the coherent relationship with matrix and the η′ phase of the semicoherent relationship with the matrix, it is necessary to have smaller grain size, larger dispersion density, and higher material strength [8, 10, 29]. In the experiment, the alloy after two-stage solution aging treatment was observed by transmission electron microscopy. As shown in Fig. 10, dispersive precipitates were present. These precipitates strengthen the alloys. It can be seen from the transmission morphology that a small amount of precipitates were also distributed at the grain boundary, which will have a certain adverse effect on the intergranular corrosion of the alloy. It is therefore necessary to study the corrosion resistance of alloys after two-stage and re-regression aging to reduce the number and size of precipitates at grain boundaries.

Conclusions

1. The composition of the experimentally prepared Al alloy was complex, and the as-cast structure exhibited obvious dendrite segregation. After two-stage homogenization annealing at 455 °C × 12 h + 475 °C × 12 h, all segregated alloying elements except a small amount of Fe-rich phase could diffuse into the matrix, and the homogenization effect was better.
2. The factors affecting the final mechanical properties were the amount of precipitated nanophase and the recrystallization degree of the matrix. When the sin-

gle-stage solution treatment was applied, the optimum process was 470 °C × 1 h. As long as the temperature was lower than that, the degree of supersaturation of the alloy decreased. This also led to a poor aging precipitation effect. However, a higher temperature will result in a higher recrystallization degree of the alloy. The phenomenon of grain growth affected the comprehensive mechanical properties.

3. The driving force of recrystallization was reduced due to the release of deformation energy of the treated two-stage solution alloys during the single-stage solution treatment at low temperature. The recrystallization degree was not obvious when the second-stage solution treatment temperature was properly increased. Meanwhile, the supersaturation of the alloy increased, the aging precipitation effect improved, and the comprehensive mechanical properties of the alloy were improved.

Author contributions JC, TL, GW, CW, RC, and DW prepared the Al-Zn-Mg-Cu-Zr-Ce alloy samples and performed the solution treatment system under the supervision of H.F. All authors discussed the results and approved the final manuscript.

Funding This research was funded by Keynote Research and Development Projects of Shandong (No. 2017CXGC0402), Key Projects of Humanities and Social Sciences Program of Colleges and Universities in Shandong (No. J17RZ011), Special Program for the Training of Young Scholars in Social Science Planning of Shandong (No. 17CQXJ03), Science and Technology Project of Colleges and Universities in Shandong (No. J18KB046), and Natural Science Foundation of Shandong Province (Grant No. ZR2017MEM009).

Conflicts of Interest The authors declare no conflicts of interest.

References

1. C. Huang, T. Zhao, F. Gao, Research development of heat-treatment process influence on microstructure and properties for 7××× series aluminum alloys. Mater. Rev. A. **29**(12), 98–102 (2015)
2. X. Zhang, Y. Deng, Y. Zhang, Development of high strength aluminum. Acta Metall. Sin. **51**(3), 257–271 (2015)
3. J. Zhao, X. Xu, Y. Chen, L. Sun, C. Tan, X. Zhang, Microstructures and properties of ultra-high-strength Al-Zn-Mg-Cu-Zr-Sr alloy with pre-deformation. Chin. J. Rare Metals. **40**(12), 1193–1199 (2016)
4. Y. Qunying, L. Wenyi, Z. Zhiqing, H. Guangjie, L. Xiaoyong, Hot deformation behavior and processing maps of AA7085 aluminum alloy. Rare Metal Mater. Eng. **47**(2), 0409–0415 (2018)
5. H. Wu, S.P. Wen, H. Huang, B.L. Li, X.L. Wu, K.Y. Gao, W. Wang, Z.R. Nie, Effects of homogenization on precipitation of Al_3(Er,Zr) particles and recrystallization behavior in a new type Al-Zn-Mg-Er-Zr alloy. Mater. Sci. Eng. A **689**, 313–322 (2017)
6. X. Da, Z. Li, G. Wang, X. Li, X. Lv, Y. Zhang, Y. Fan, B. Xiong, Phase transformation and microstructure evolution of an ultra-high strength Al-Zn-Mg-Cu alloy during homogenization. Mater. Charact. **131**, 285–297 (2017)
7. H. Lin, L. Ye, L. Sun, T. Xiao, S. Liu, Y. Deng, X. Zhang, Effect of three-step homogenization on microstructure and properties of 7N01 aluminum alloys. Trans. Nonferrous Met. Soc. China **28**, 829–838 (2018)
8. F. Wang, W. Meng, H. Zhang, Z. Han, Effects of under-aging treatment on microstructure and mechanical properties of squeeze-cast Al-Zn-Mg-Cu alloy. Trans. Nonferrous Met. Soc. China **28**, 1920–1927 (2018)
9. S. Sun, P. Liu, H. Jiaying, C. Hong, X. Qiao, S. Liu, R. Zhang, W. Chengge, Effect of solid solution plus double aging on microstructural characterization of 7075 Al alloys fabricated by selective laser melting (SLM). Opt. Laser Technol. **114**, 158–163 (2019)
10. L. Wan, Y.-L. Deng, L.-Y. Ye, Y. Zhang, The natural ageing effect on pre-ageing kinetics of Al-Zn-Mg alloy. J. Alloys Compd. **776**, 469–474 (2019)
11. Z. Zhang, J. Yu, D. He, Influence of contact solid-solution treatment on microstructures and mechanical properties of 7075 aluminum alloy. Mater. Sci. Eng. A **743**, 500–503 (2019)
12. F. Hongjie, S. Jie, W. Hongbo, Y. Dengfeng, Effects of trace of Ce element on microstructure and properties of 7136 aluminum alloy. J. Chin. Soc. Rare Earths **34**(3), 313–319 (2016)
13. J. Sun, H. Fang, H. Liu, C. Shi, Effect of trace rare earth Ce on microstructure and properties of 7085 aluminum alloy. J. Chin. Soc. Rare Earths **35**(4), 501–507 (2017)
14. K.G. Krishna, K. Sivaprasad, K. Venkateswarlu, K.C. Hari Kumar, Microstructural evolution and aging behavior of cryorolled Al-4Zn-2 Mg alloy. Mater. Sci. Eng. A **535**, 129–135 (2012)
15. K.S. Ghosh, N. Gao, M.J. Starink, Characterisation of high pressure torsion processed 7150 Al-Zn-Mg-Cu alloy. Mater. Sci. Eng. A **552**, 164–171 (2012)
16. R. Ghiaasiaan, X. Zeng, S. Shankar, Controlled Diffusion Solidification (CDS) of Al-Zn-Mg-Cu (7050): microstructure, heat treatment and mechanical properties. Mater. Sci. Eng. A **594**, 260–277 (2014)
17. N. Yazdian, F. Karimzadeh, M. Tavoosi, Microstructural evolution of nanostructure 7075 aluminum alloy during isothermal annealing. J. Alloys Compd. **493**, 137–141 (2010)
18. D.K. Xu, N. Birbilis, D. Lashansky, P.A. Rometsch, B.C. Muddle, Effect of solution treatment on the corrosion behaviour of aluminium alloy AA7150: optimization for corrosion resistance. Corros. Sci. **53**, 217–225 (2011)
19. X.M. Li, M.J. Starink, Identification and analysis of intermetallic phases in overaged Zr-containing and Cr-containing Al-Zn-Mg-Cu alloys. J. Alloys Comp. **509**, 471–476 (2011)
20. H. Lia, P. Chen, Z. Wang, F. Zhu, R. Song, Z. Zheng, Tensile properties, microstructures and fracture behaviors of an Al-Zn-Mg-Cu alloy during ageing after solution treating and cold-rolling. Mater. Sci. Eng. A **742**, 798–812 (2019)
21. H. Li, F. Cao, S. Guo, Y. Ji, D. Zhang, Z. Liu, P. Wang, S. Scudino, J. Sun, Effects of Mg and Cu on microstructures and properties of spray-deposited Al-Zn-Mg-Cu alloys. J. Alloys Compd. **719**, 89–96 (2017)
22. G. Kaixuan, K. Wang, L. Chen, J. Guo, C. Cui, J. Wang, Microplastic deformation behavior of Al-Zn-Mg-Cu alloy subjected to cryocycling treatment. Mater. Sci. Eng. A **742**, 672–679 (2019)
23. S. Qu, M. Li, C. Shi, H. Fang, J. Sun, Homogenizing and solution of Al-8.0Zn-2.3Cu-2.0 Mg-0.2Zr aluminum alloy. Heat Treat. Metals **42**(6), 114–118 (2017)
24. F. Zhang, X. Wang, W. Yuan, C. Yang, Effects of solution time on microstructures, and properties of 7050 aluminum alloy. J. Hunan Univ. (Nat. Sci.) **45**(12), 11–14 (2018)
25. R. Zhu, Y. Zhang, B. Xiong, Z. Li, X. Li, H. Liu, B. Zhu, F. Wang, Effect of solution treatment on microstructures and mechanical properties of 7136 aluminum alloy. J. Aeronaut. Mater. **32**(5), 37–42 (2012)

26. W. Sun, Y. Zhang, X. Li, Z. Li, F. Wang, H. Liu, B. Xiong, Effect of solution treatment on microstructures and mechanical properties of 7136 aluminum alloy. J. Aeronaut. Mater. **34**(3), 35–41 (2014)
27. X. Zhou, Y. Sun, Y. Zhang, W. Wang, Y. He, J. Fu, J. He, Effect of homogenizing treatment on microstructure and mechanical properties of as-cast Al-Mg-Si-Cu alloy. Heat Treat. Met. **42**(6), 93–96 (2017)
28. A. Rollett, *Recrystallization and Related Annealing Phenomena* (Elsevier, Amsterdam, 1995)
29. L.L. Liu, Q.L. Pan, X.D. Wang, S.W. Xiong, The effects of aging treatments on mechanical property and corrosion behavior of spray formed 7055 aluminium alloy. J. Alloys Compd. **735**, 261–276 (2018)